Revision

7th June 2015

Boron-Doped Diamond Dual-Plate Deep-Microtrench Device for Generator-Collector Sulfide Sensing

Harriet M. Harvey [a], Andrew J. Gross [a], Paula Brooksby [b], Alison J. Downard [b], Stephen J. Green [c], C. Peter Winlove [c], Nigel Benjamin [d], Paul G. Winyard [d], Matthew Whiteman [d], Jules L. Hammond [e], Pedro Estrela [e], and Frank Marken *[a]

[a] *Department of Chemistry, University of Bath, Bath, BA2 7AY, UK*
[b] *Department of Chemistry, University of Canterbury, MacDiarmid Institute for Advanced Materials & Nanotechnology, Christchurch 8140, New Zealand*
[c] *Department of Physics, College of Engineering, Mathematics and Physical Sciences, University of Exeter, Stocker Road, Exeter, EX4 4QL, UK*
[d] *University of Exeter Medical School, University of Exeter, St Luke's Campus, Exeter, EX1 2LU, UK*
[e] *Department of Electronic & Electrical Engineering, University of Bath, Bath, BA2 7AY, UK*

To be submitted to Electroanalysis

Proofs to F. Marken

F.Marken@bath.ac.uk

Abstract

A BDD-BDD dual-plate microtrench electrode with 6 μm inter-electrode spacing is investigated using generator-collector electrochemistry and shown to give microtrench depth-dependent sulfide detection down to the μM levels. The effect of the microtrench depth is compared for a "shallow" 44 μm and a "deep" 180 μm microtrench and linked to the reduction of oxygen to hydrogen peroxide which interferes with sulfide redox cycling. With a deeper microtrench and a fixed collector potential at -1.4 V vs. SCE, two distinct redox cycling potential domains are observed at 0.0 V vs. SCE (2-electron) and at 1.1 V vs. SCE (6-electron).

Keywords: chloride, serum, seawater, inflammation, feedback, sensing, voltammetry.

Graphical Abstract:

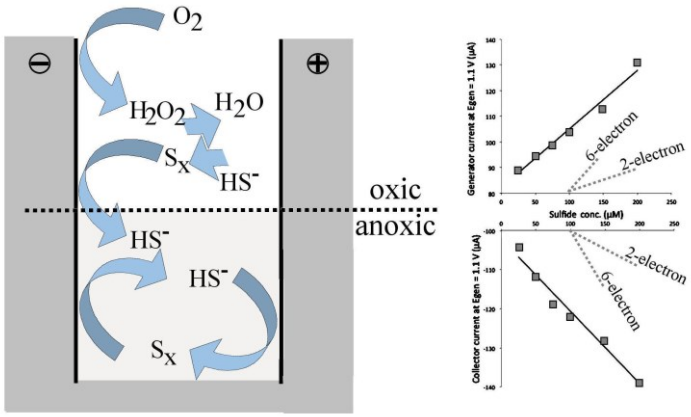

1. Introduction

Dual-plate microtrench electrode systems (Figure 1) are based on two closely-spaced planar electrodes with a gap size of 1-10 μm to allow fast inter-electrode diffusion and feedback amplification for redox cycleable processes [1,2]. Due to dual-potential control and removal of irreversible redox processes [3], these electrodes are promising for investigating electro-analytical processes with recent examples in nitrate/nitrite detection in serum [4], cysteine/cysteine [5] and chloride/chlorine detection in buffer media [6], nitrobenzene [7] and proton [8] detection, as well as applications involving non-electrochemically active anions such as phosphate [9] in oil-filled liquid|liquid microtrench systems. Here a boron-doped diamond (BDD) dual-plate microtrench electrode is employed for the detection of sulfide.

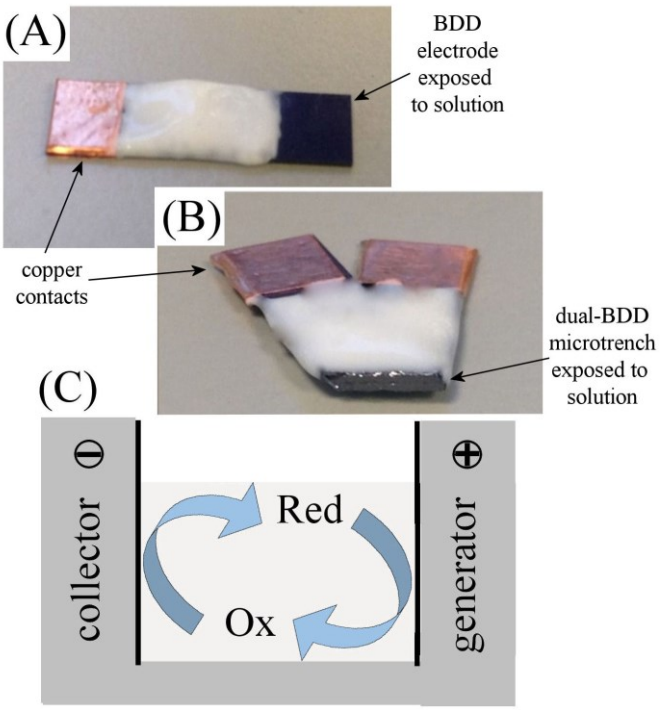

Figure 1. Photographs of (A) a BDD plate electrode and (B) a BDD dual-plate microtrench electrode. (C) Schematic drawing of the redox cycling mechanism.

Hydrogen sulfide (H_2S) is a colourless, flammable and toxic gas that is produced endogenously in mammalian tissues from L-cysteine [10] with numerous biological signalling functions [11,12]. Brain H_2S has been recognised as playing a role (anti-inflammatory) in the progression of central nervous system diseases such as Alzheimer's [13] and Parkinson's [14] disease. Additionally, H_2S levels have been found to be disrupted in many other disease states including renal diseases [15] and diabetes [16,17]. Furthermore, H_2S releasing compounds have been developed and pre-clinically tested as a novel therapeutic class of cyto-protective and anti-inflammatory agents [18]. The detection of H_2S or HS^- *in situ,* for example in biological fluids during therapy, remains a very challenging task in particular at the sub-micro-molar level. Therefore, new detection methods are needed.

The most widely used technique to determine H_2S levels in serum and plasma is a spectrophotometric technique based on the indirect measurement of the indicator dye methylene blue. The assay involves the temporary "capture" of aqueous sulfide with a metal, commonly zinc acetate to yield a stable metal sulfide. This capture step avoids the loss of sulfide via volatilisation or air oxidation. Subsequent acidification releases the sulfide to react with *N*,*N*-dimethyl-*p*-phenylenediamine (DMPD) and iron chloride ($FeCl_3$), generating methylene blue which is readily measured using a spectrophotometer at 670 nm [19]. Related voltammetric methods have been suggested where the methylene blue derivative gives a characteristic signal change in the presence of sulfide [20,21,22,23]. Polarographic H_2S sensors can be highly sensitive but are often hampered by effects from complex biological media [24]. Highly regarded for the simplicity in application and relatively low cost, fluorescent

based methods for H_2S detection have been developed [25]. A promising fluorescent H_2S probe has been proposed which is functional in blood plasma with moderate detection sensitivity [26]. Additionally, chromatography methods have been reported including ion chromatography [27], and gas chromatography with chemiluminescence [28].

Electrochemical methods for sensing gaseous H_2S have been demonstrated in laboratory devices [29,30,31,32,33], as well as electrocatalytic or stripping voltammetry devices for sulfide in solution [34,35] and in seawater [36]. A nickel electrode has been shown to give good sulfide detection in alkaline media [37]. However, there are few examples of successful electrochemical detection of H_2S in biological matrices. Sulfide-specific ion-selective electrodes (ISEs) have been developed for measurements in biological samples with detection limits of 1-10 μM but they suffer from problems with interferences. Erroneous results have been observed, for example, due to the alkaline conditions required for testing [38]. For the amperometric detection the redox mechanism in hydrogen sulfide sensing can be based on the 2-electron oxidation to sulfur, which is affected by pH (for H_2S pK_{A1} = 6.9 and pK_{A2} = 14.1). Bitziou and co-workers [39] employed a dual-band BDD flow electrode with 200 μm inter-electrode gap separation for H_2S detection in aqueous solutions. The electrochemical setup involved an upstream BDD generator electrode which is used to generate hydroxide ions from water electrolysis to locally change the pH of the downstream BDD collector electrode, making the solution more alkaline (within the pH 7-14 region) for the direct oxidation of HS^-. A recent electrochemical study by Aziz and coworkers [40] focused on sulfide sensing at metal oxide

conducting electrode materials such as tin-doped indium oxide (ITO), fluorine-doped tin oxide (FTO), aluminium-doped zinc oxide (AZO), and gallium-doped zinc oxide (GZO). ITO provided the best results yielding a linear sulfide concentration response in the range of 50-350 μM, with fast electrode response and good selectivity and sensitivity for sulfide in the presence of excess Na_2SO_3, Na_2SO_4, or NaCl. The ITO electrode material also showed significant resistance to sulfide poisoning with little difference between the responses for a fresh electrode and an electrode that had been used 50 times. It was also noted that a second more positive oxidation peak was present which was attributed to further oxidation of S^0 or S^{2-} to sulfite (SO_3^{2-}) and/or sulfate (SO_4^{2-}). The true levels of hydrogen sulfide in biological tissue or serum are still under discussion. These may be quite low (sub micromolar), and in conjunction with the sulfide reactivity towards oxygen, they therefore pose a very challenging analytical target [41].

In this study the concept of redox cycling for HS^- detection (and thereby amplifying the sensor signal) is investigated in a dual-plate BDD-BDD microtrench electrode system. It is shown that the redox cycling and detection of sulfide are possible in the presence of ambient oxygen levels and that the microtrench depth plays an important role in the overall redox cycling mechanism. It is suggested that removal of oxygen occurs *in situ* in the upper region of the dual-plate electrode, adjacent to the bulk solution. The lower or "deeper" region of the microtrench is important for the analytical sulfide response.

2. Experimental

2.1. Reagents

Sodium phosphate monobasic monohydrate, sodium phosphate dibasic heptahydrate, potassium chloride, sodium hydroxide pellets, potassium nitrate, sodium sulfate, sodium sulfide nonahydrate, sodium chloride, hexaammineruthenium(III)chloride and Kolliphore®EL were purchased from Sigma Aldrich (UK) and used without further purification. All solutions were prepared with demineralised water with a resistivity of not less than 18 MΩ cm.

2.2. Instrumentation

Electrochemical measurements were performed at 20 ± 2 ºC using either a PGSTAT12 bipotentiostat system (Autolab, EcoChemie, Netherlands) or a SP-300 bipotentiostat system (Biologic, France). A platinum wire counter electrode and saturated calomel electrode reference (SCE, Radiometer) were used throughout the study. A PWM32 spin coater (Headway) was used to spin photoresist during microtrench electrode fabrication. Scanning electron microscopy (SEM) images were obtained with a JSM-6480LV (JEOL, Japan).

2.3. Electrode Fabrication and Calibration

The BDD single electrode was prepared using a 5 mm × 20 mm BDD-coated p-doped Si substrate (300 nm BDD, SiO_2/Si_3N_4 interlayer, 8000 ppm doping and resistivity = 10 mΩ cm, purchased from NeoCoat SA, Switzerland). A copper contact was applied to one end of the substrate using conducting copper tape (RS) and a 5 mm^2 area defined at the other end by application of silicone (Silcoset 151, Farnell, UK) (Figure 1).

For fabrication of the BDD-BDD dual-plate microtrench electrode a technique previously described [6] was employed. Two 5 mm × 20 mm BDD electrodes were rinsed with demineralised water, acetone and isopropyl alcohol and dried with a stream of nitrogen. A region of approximately 5 mm × 5 mm for electrical contact was masked with Kapton tape (Farnell, UK) before the substrates were spin-coated with one coat of SU-8 2002 photoresist at 500 rpm for 15 seconds and 3000 rpm for 30 seconds. The Kapton tape was then removed and the two substrates were pressed together vis-à-vis and placed on a hot plate at 90 °C for 2 minutes before the temperature was ramped up to 160 °C for 5 minutes. Once cooled to room temperature, the end of the BDD electrode was sliced off with a diamond cutter (Isomet 1000, Buehler) and polished flat with SiC abrasive paper (Buehler). The SU-8 photoresist layer in-between the substrates was then partially etched using piranha solution (5:1 sulfuric acid: hydrogen peroxide; *caution: this is a highly aggressive solution and should be prepared and handled with care*) to form the trench. Copper tape was then applied to make electrical contact with the working electrodes. Figure 2 shows typical microtrench electron micrographs.

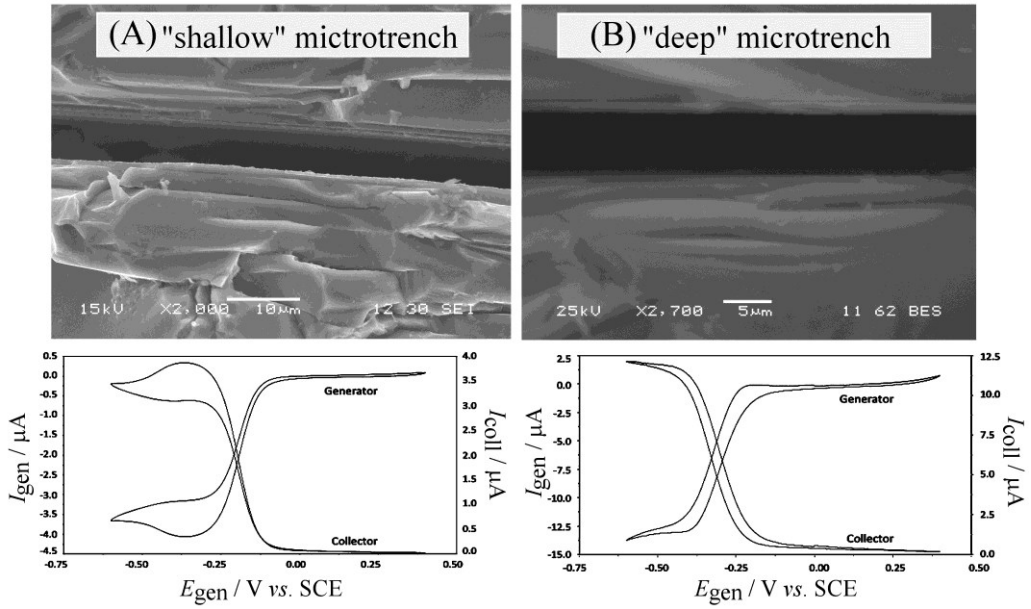

Figure 2. SEM images of the BDD-BDD microtrench junctions for (A) the shallow microtrench and (B) the deep microtrench. Also shown are generator-collector voltammograms (scan rate 80 mVs^{-1}; E_{coll} 0.3 V vs. SCE) for 1 mM $Ru(NH_3)_6^{3+}$ in 0.1 M NaCl. The collector limiting current is mass transport controlled and allows the microtrench depth to be estimated (see text).

A solution of 1 mM $Ru(NH_3)_6^{3+/2+}$ redox couple in 0.1 M NaCl supporting electrolyte was utilised to estimate the microtrench depth (Figure 2). Limiting currents recorded at the collector electrode and measured at E_{gen} -0.5 V vs. SCE are 3.2 µA for the shallow and 13 µA for the deeper microtrench. The expression for the Nernst diffusion layer steady state case, trench depth = $\frac{I_{lim} \times \delta}{nFDwc}$ [42], can then be employed. SEM images (Figure 2.) of the two BDD-BDD microtrench electrodes were recorded and reveal the same trench widths of δ = 6 µm. The number of transferred electrons (n) is 1 for $Ru(NH_3)_6^{3+}$, the diffusion coefficient (D) is 9.1 × 10^{-10} m^2 s^{-1} [43], the electrode width (w) is 5 mm, and the concentration (c) is 1 mol m^{-3}. The approximate microtrench depths were estimated to be 44 ± 4 µm ("shallow" electrode), and 180 ± 20 µm ("deep" electrode).

3. Results and Discussion

3.1. Voltammetry at a BDD Single Plate Sensor: Sulfide Detection in Aerated Solution

Sulfide electrochemistry was first investigated at a single boron-doped diamond electrode immersed in 20 mM phosphate buffer pH 8 with 0.1 M KNO_3 as supporting electrolyte and 4 mM Kolliphor®EL as an additive to improve the solubility of elemental sulfur. Consecutive cyclic voltammograms were recorded commencing at -0.4 V and scanning positive to +1.5 V, then negative to -1.6 V vs. SCE (Figure 3A). The background response clearly shows a reduction peak at -1.2 V vs. SCE (see P1, equation 1) corresponding to the reduction of oxygen. This process on BDD is likely to be associated here with the formation of hydrogen peroxide [44].

P1: $O_2(aq) + 2\,H^+(aq) + 2\,e^- \rightarrow H_2O_2(aq)$ (1)

In the presence of 1 mM sulfide, a well-defined oxidation peak is observed at +1.1 V vs. SCE in both the first and second potential cycle (Figure 3A, process P3). A further oxidation peak becomes apparent only during the second potential cycle at -0.1 V vs. SCE (Figure 3A, process P2). It is speculated that this (surface sensitive) secondary peak results from the chemically irreversible 2-electron oxidation of HS^- (equation 2) whereas the peak at +1.1 V vs. SCE may be caused by the further oxidation of the sulfide species to sulfite SO_3^{2-} (equation 3) or eventually sulfate SO_4^{2-}.

P2: $HS^-(aq) \rightarrow 1/x\,S_x(aq) + H^+(aq) + 2\,e^-$ (2)

P3: $HS^-(aq) + 3\,H_2O \rightarrow SO_3^{2-}(aq) + 7\,H^+(aq) + 6\,e^-$ (3)

Figure 3B shows cyclic voltammograms for the second potential cycle recorded at 100 mVs^{-1} over the potential range -1.6 V to +1.5 V vs. SCE for increasing concentrations of sulfide. An increase in peak current is observed for the oxidation wave at +1.1 V vs. SCE with increasing sulfide concentration from 0 to 2 mM consistent with literature reports [37,45]. The oxidation wave becomes more pronounced upon increasing sulfide concentration and the plot of peak current versus sulfide concentration is linear (Figure 3B, inset). A reduction process under similar conditions has been reported in the literature [35] at negative potentials close to ca. -1.5 V vs. SCE corresponding to the back-reduction of sulfur deposits back to sulfide, but this is not observed here possibly due to (i) the presence of ambient oxygen or (ii) the Kolliphor®EL binding and solubilisation of sulfur. Figure 3C shows that the oxidation-based methodology is sensitive to sulfide levels at lower micromolar levels. The process P2 that is observed usually during the second potential cycle is not well-resolved below 1 mM sulfide. A sulfur nucleation overpotential and electrode surface modification could be associated with this process, but also a change in the diamond surface termination [46] after scanning into the negative potential range cannot be ruled out as the cause.

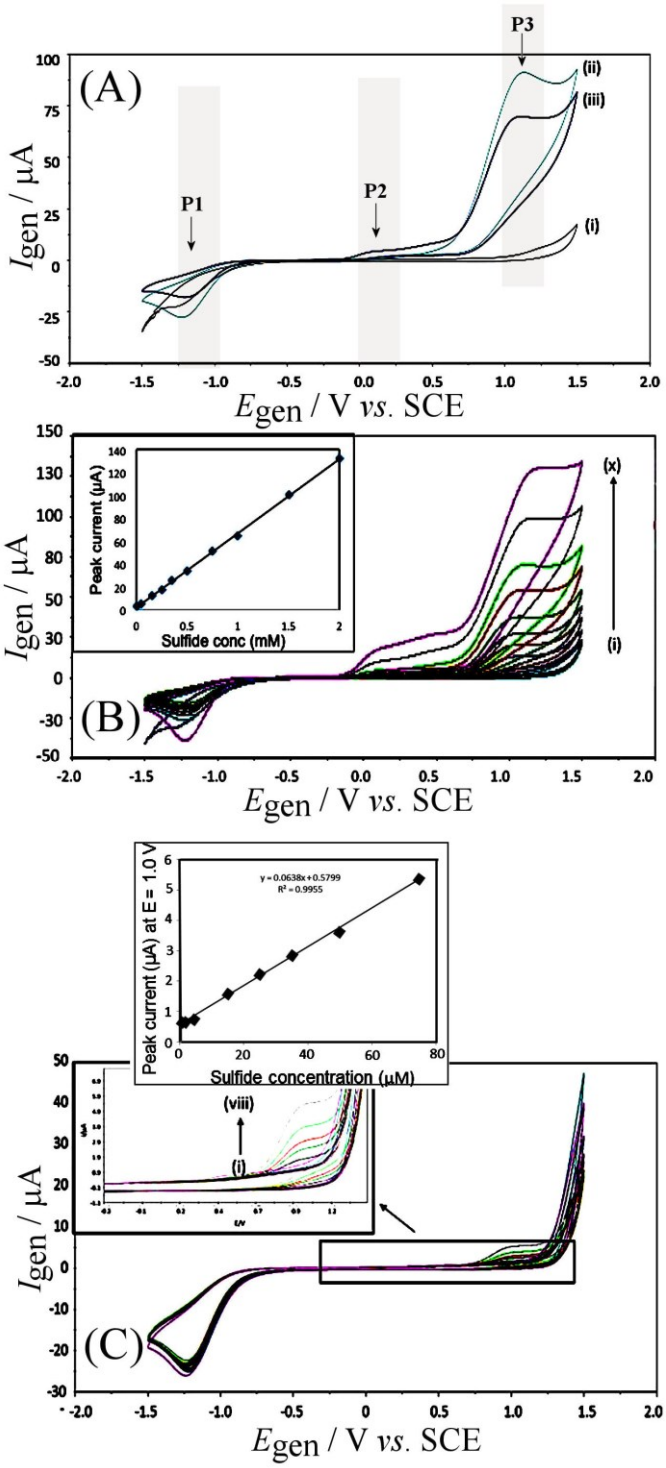

Figure 3. (A) Cyclic voltammograms (scan rate 100 mVs^{-1}) recorded at a single BDD electrode in 20 mM phosphate buffer pH 8/0.1 M KNO_3/4 mM Kolliphor®EL (i) in the absence of sulfide, and (ii) scan 1 and (iii) scan 2 in the presence of 1 mM sulfide. (B) As above but for (i) 0.00 mM, (ii) 0.05 mM, (iii) 0.15 mM, (iv) 0.25 mM, (v) 0.35 mM, (vi) 0.50 mM, (vii) 0.75 mM, (viii) 1.0 mM, (ix) 1.5 mM, and (x) 2.0 mM sulfide (inset: plot of sulfide concentration versus peak current measured at 1.1 V vs. SCE). (C) As above but for (i) 0.5 µM, (ii) 1.0 µM, (iii) 5.0 µM, (iv) 15 µM, (v) 25 µM, (vi) 35 µM, (vii) 50 µM, and (viii) 75 µM sulfide (inset: plot of sulfide concentration versus peak current measured at 1.1 V vs. SCE).

3.2. Voltammetry at a BDD-BDD Dual Plate Sensor I.: Sulfide Signals in a Shallow Microtrench

The shallow BDD-BDD microtrench electrode is employed first to explore the potential window and parameters for sulfide sensing. Figure 4 shows typical generator-collector voltammetry data obtained using a collector potential of -1.4 V vs. SCE. Although typical sulfide oxidation responses are observed at the generator, more positive collector potential settings did not provide any sulfide dependent collector current responses. However, perhaps surprisingly, at E_{coll} = -1.4 V vs. SCE the collector current became more negative with increasing sulfide concentration. At this rather negative potential the collector electrode process is dominated by oxygen reduction (see process P1 in Figure 3). For this case, the presence of sulfide appears to increase the reduction current for oxygen; that is, sulfide can catalyse the reduction of oxygen beyond hydrogen peroxide under these conditions. The process is summarised by the schematic in Figure 4B.

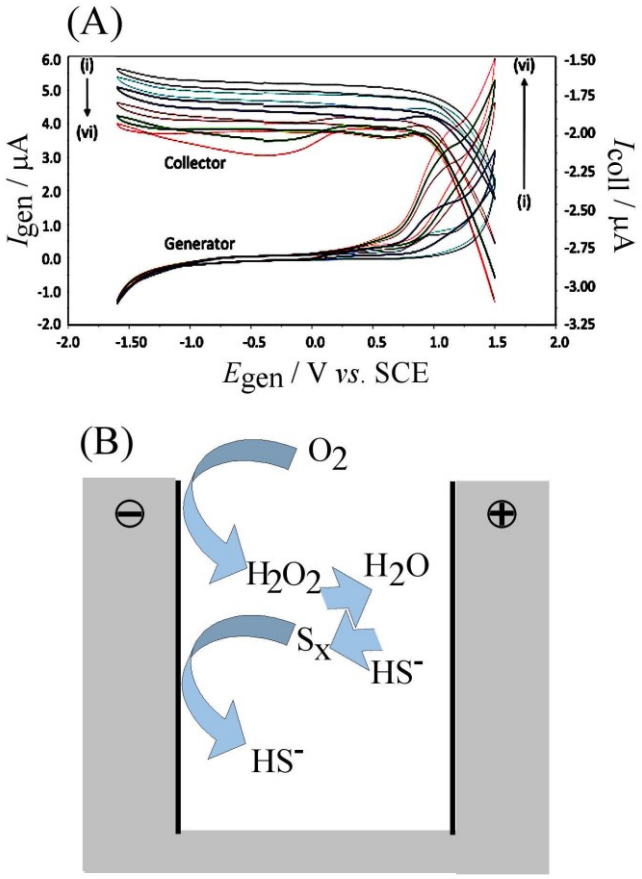

Figure 4. (A) Generator and collector voltammograms recorded at a shallow BDD-BDD microtrench electrode in 20 mM phosphate buffer pH 8/0.1 M KNO_3/4 mM Kolliphor®EL with collector potential fixed at -1.4 V (vs. SCE) in (i) 0.0 mM, (ii) 0.5 mM, (iii) 1.0 mM, (iv) 1.5 mM, (v) 2.0 mM, and (vi) 2.5 mM sulfide. All scans recorded at 100 mVs^{-1} in ambient oxygen. (B) Schematic depiction of the mechanism inside the microtrench.

Both the generator and collector voltammograms recorded at the shallow electrode display a sulfide concentration dependant current signal. The generator signals are similar to those recorded at the single BDD electrode, with a well-defined peak current observed at +1.1 V vs. SCE. There seems to be no clear sulfide-related feedback current at the collector electrode at E_{gen} = +1.1 V vs. SCE. Rather, all of the collector current voltammograms are shifted increasingly negative with increasing sulfide levels. The scheme in Figure 4B provides a tentative mechanism for this observation based on a sulfide catalysed hydrogen peroxide reduction. The

"waviness" of the collector response at higher sulfide concentrations is indicative of further complexity and the current is unlikely to be beneficial for sensing applications. Therefore, a deeper microtrench electrode system was prepared and is investigated next.

3.3. Voltammetry at a BDD-BDD Dual Plate Sensor II.: Sulfide Signals in a Deep Microtrench

Generator-collector voltammograms obtained using a 180 μm deep BDD dual-plate microtrench electrode are shown in Figure 5. The voltammograms, at first sight, appear to reveal a response very different from that seen with the shallow electrode. The generator and collector signals are more symmetrical, suggesting the sulfide redox active species detected is now continually redox-cycled by oxidation at the generator and back-reduction at the collector. The generator voltammograms obtained in the presence of sulfide show an increase in current, when compared to the blank, from generator potential -0.75 V vs. SCE to 1.5 V vs. SCE (Figure 5A). Furthermore, there are two slight oxidation waves commencing at approximately -0.5 V vs. SCE and +0.5 V vs. SCE. The collector electrode mirrors this response as the oxidised species are subsequently reduced at the collector. It seems likely that the first redox cycle is caused by HS^- oxidation to S^0 with the second redox cycle being associated with further oxidation to SO_3^{2-} and/or SO_4^{2-}. The underlying negative shift of the collector response seen in the shallow trench device does still occur but remains insignificant under these conditions.

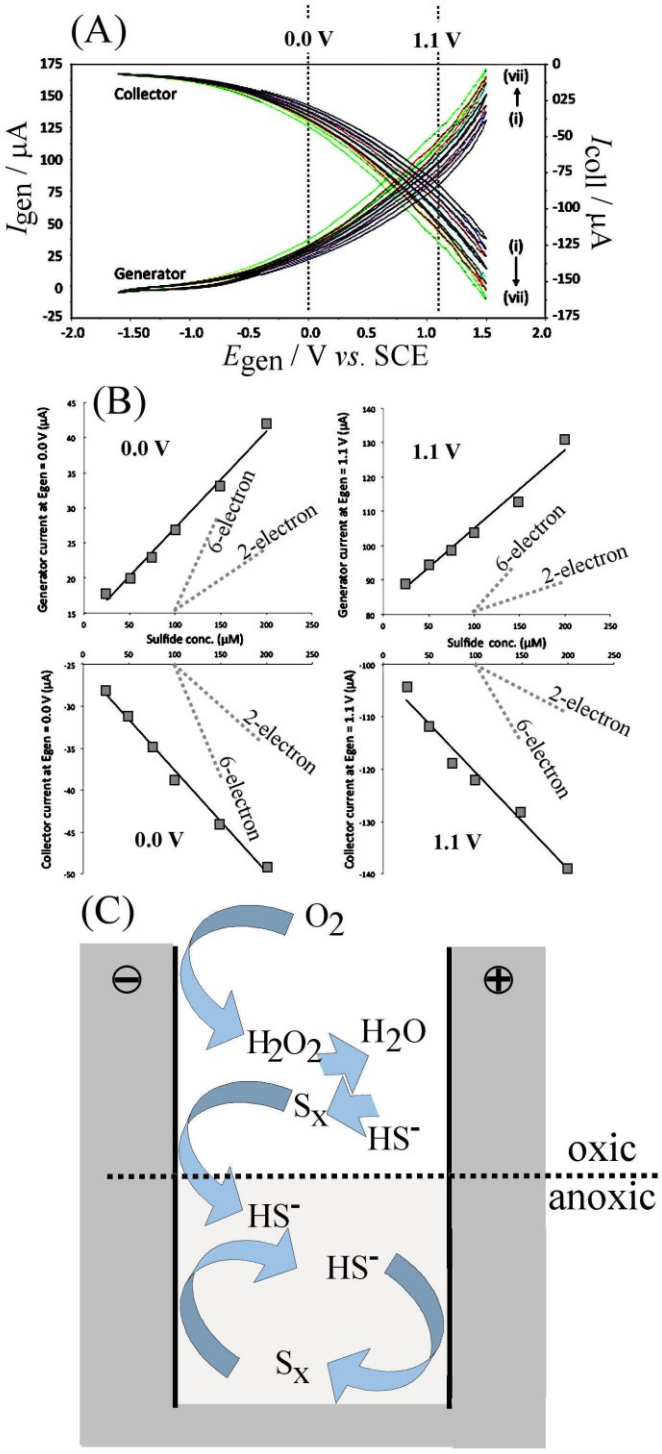

Figure 5. (A) Generator and collector voltammograms recorded at a deep BDD-BDD microtrench electrode in 20 mM phosphate buffer pH 8/0.1 M KNO_3/4 mM Kolliphor®EL, with collector potentials fixed at -1.4 V vs. SCE in (i) 0.00 mM, (ii) 0.25 mM, (iii) 0.50 mM, (iv) 0.75 mM, (v) 1.00 mM, (vi) 1.50 mM and (vii) 2.00 mM sulfide. All scans recorded at 100 mVs^{-1} in ambient oxygen. (B) Plots of generator currents (top) and collector currents (bottom) versus sulfide concentration measured at E_{gen} = 0.0 V and E_{gen} = 1.1 V vs. SCE. (C) Schematic summary of the mechanism inside the microtrench.

Current readings were taken at E_{gen} = 0.0 V and at 1.1 V vs. SCE as a function of the sulfide concentration. Plots in Figure 5B show linear trends. The slope of these plots can be interpreted in terms of the Nernst diffusion layer model [47] with only the parameter n (the number of electrons transferred per molecule diffusing to the electrode surface) unknown (equation 4).

$$\frac{dI}{dc} = n \times \frac{FDA}{\delta} \tag{4}$$

For a microtrench with δ = the trench width, 6 μm, A= the area calculated from depth and width, 0.18 mm × 5 mm, F = Faraday constant, and D = the diffusion coefficient, 1.6×10^{-9} m^2s^{-1} for hydrogen sulfide [48], the theoretical slope for a 2-electron or a 6-electron process can be estimated (see Figure 5B). The slopes for the process at E_{gen} = 0.0 V vs. SCE (Figure 5B), in particular for the collector current, appear reasonably close to the 2-electron case, suggesting that process P2 (equation 2) is indeed dominating at this potential. However, there is uncertainty in the remaining effects of oxygen and also the unknown rate of diffusion for the oxidised forms of sulfide. The slopes obtained at E_{gen} = 1.1 V vs. SCE (Figure 5B) are clearly increased although still not quite consistent with that expected for a 6-electron process (equation 3, P3). Therefore, other intermediates may be involved with further complexity in the overall redox cycle mechanism.

One conclusion from these microtrench generator-collector voltammetry measurements is that detection of sulfide is feasible and in particular at a very mild potential of 0.0 V vs. SCE and in the presence of ambient levels of oxygen. Healthy human blood has been suggested to contain H_2S levels of possibly up to ~60 μM [49] with higher or lower concentrations possibly associated with certain disease states, although the speciation of sulfide and actual "free" sulfide levels are still debated. The preliminary data in Figure 5B suggests that measurements in the 60 μM range are achievable, especially with further device improvements such as an even deeper trench and a smaller inter-electrode gap.

3.4. Voltammetry at a BDD-BDD Dual Plate Sensor III.: Sulfide Sensing Protocol

In order to demonstrate a standard addition test methodology, four standard additions of 25 μM sulfide were added to a cell solution containing 20 mM phosphate buffer pH 8, 0.1 M KNO_3, and 4 mM Kolliphor®EL, before and after the addition of an "unknown" sulfide sample (here a 50 μM test amount). Voltammograms were recorded at each addition step and revealed an obvious increase in current response with sulfide addition as expected (Figure 6A). The current signals at E_{gen} = 0.0 V and +1.1 V vs. SCE for both generator and collector electrodes were evaluated and plotted versus standard addition concentration (Figure 6B), omitting the values for the "unknown" sample. Two linear plots (before and after unknown sample) were obtained and the horizontal half-way point between the two trend lines were obtained and used to extrapolate to the "unknown" sample concentration. The estimated concentration of the unknown addition ranged from 45-54 μM, with an averaged estimated concentration of 51 μM. The actual value of the unknown spike was 50 μM and therefore the estimated values from the plots are in good agreement.

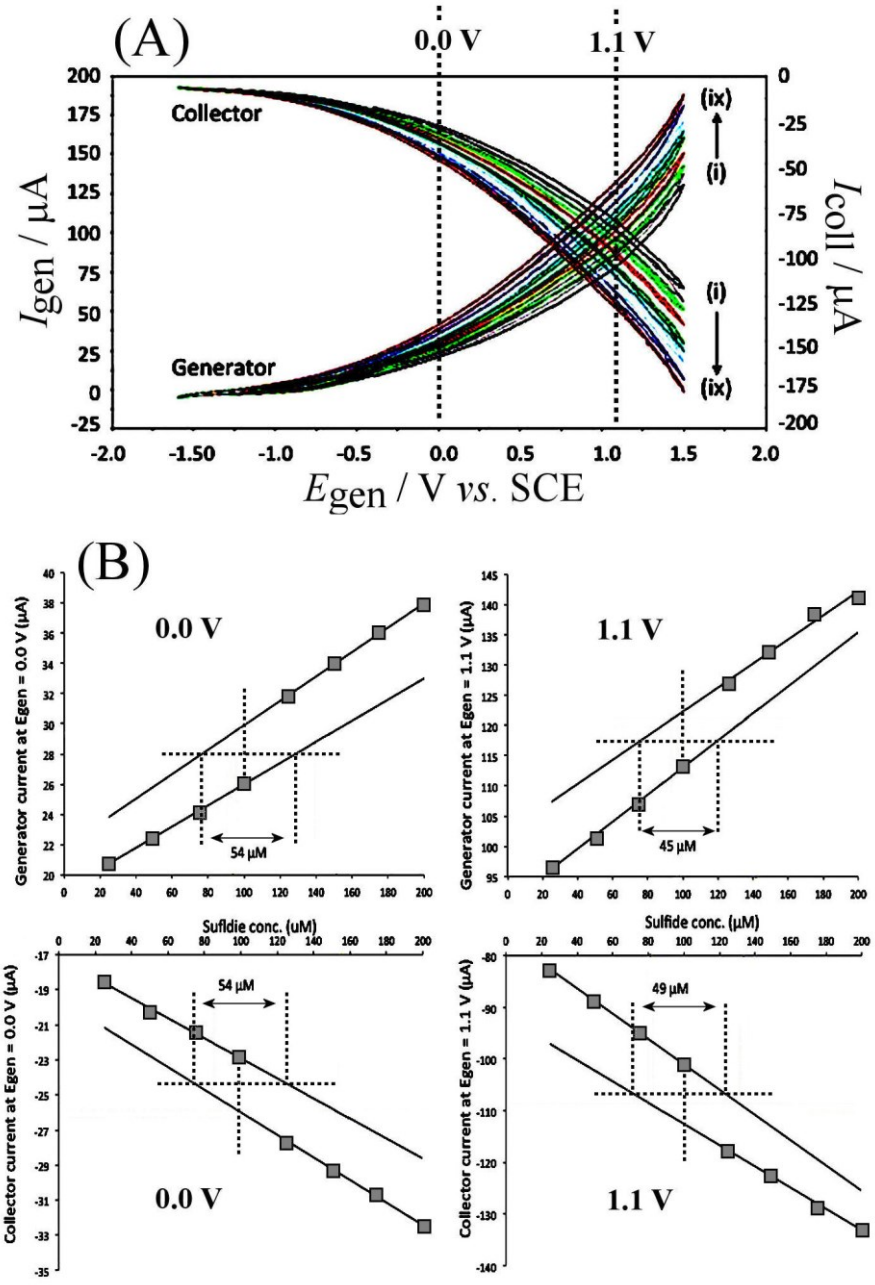

Figure 6. (A) Generator and collector voltammograms (scan rate 100 mVs^{-1}, E_{coll} -1.4 V vs. SCE) recorded at a deep BDD-BDD microtrench electrode in 20 mM phosphate buffer pH 8/0.1 M KNO_3/4 mM Kolliphor®EL with additions of (i) 25 µM, (ii) 25 µM, (iii) 25 µM, (iv) 25 µM, (v) "unknown", (vi) 25 µM, (vii) 25 µM, (viii) 25 µM, and (ix) 25 µM. (B) Plots of generator and collector currents at E_{gen} = 0.0 V and at E_{gen} = 1.1 V vs. SCE versus sulfide concentration with one unknown addition (see text).

4. Conclusions

It has been shown in this exploratory proof-of-principle study that sulfide detection in aqueous phosphate buffer media in the presence of oxygen is possible in deep dual-plate BDD-BDD microtrench electrode systems. The collector electrode can be operated at fixed potential at -1.4 V vs. SCE in order to (i) remove oxygen and to create anoxic conditions and (ii) recycle HS^- from oxidation products in a redox feedback loop. The generator electrode was scanned in a potential window from -1.6 to 1.5 V vs. SCE and two distinct redox cycle feedback regions based on a close to 2-electron process and a close to 6-electron process were revealed. Due to the mild conditions for 2-electron feedback (observed at 0.0 V vs. SCE) many interferences are likely to be less of a problem and selective sulfide sensing may be possible. For example, volatile organo-thiols such as methyl-mercaptan are known interferents in single-electrode redox mediator-based sensors, but should behave distinctly different in dual-electrode redox cycle-based sensors. However, considerable further work will be required exploring (i) microtrench geometry parameters (smaller inter-electrode distance to increase amplification and deeper trench to increase signal), (ii) reproducibility for a bigger set of devices, and (iii) interferences (in particular effects from biological matrix or serum will be of interest) to improve this new methodology for practical sulfide sensing applications *in situ* or *ex situ*, for example in blood serum.

Acknowledgements

F.M. and A.J.G. thank EPSRC for financial support (EP/I028706/1).

References

[1] E.O. Barnes, G.E.M. Lewis, S.E.C. Dale, F. Marken, and R.G. Compton, *Analyst*, **2012**, *137*, 1068-1081.

[2] S.E.C. Dale, and F. Marken, *Specialist Periodical Reports Electrochemistry*, **2014**, *12*, 132-154.

[3] M.A. Hasnat, A.J. Gross, S.E.C. Dale, E.O. Barnes, R.G. Compton, and F. Marken, *Analyst*, **2014**, *139*, 569-575.

[4] A.J. Gross, S. Holmes, S.E.C. Dale, M.J. Smallwood, S.J. Green, C.P. Winlove, N. Benjamin, P.G. Winyard, and F. Marken, *Talanta*, **2015**, *131*, 228-235.

[5] J.L. Hammond, A.J. Gross, P. Estrela, J. Iniesta, S.J. Green, C.P. Winlove, P.G. Winyard, N. Benjamin, and F. Marken, *Anal. Chem.*, **2014**, *86*, 6748-6752.

[6] A.J. Gross, and F. Marken, *Electrochem. Commun.*, **2014**, *46*, 120-123.

[7] G.E.M. Lewis, S.E.C. Dale, B. Kasprzyk-Hordern, A.T. Lubben, E.O. Barnes, R.G. Compton, and F. Marken, *Phys. Chem. Chem. Phys*., **2014**, *16*, 18966-18973.

[8] S.E.C. Dale, A. Vuorema, M. Sillanpää, J. Weber, A.J. Wain, E.O. Barnes, R.G. Compton, and F. Marken, *Electrochim. Acta*, **2014**, *125*, 94-100.

[9] M. Li, G.E.M. Lewis, T.D. James, Y.T. Long, B. Kasprzyk-Hordern, J.M. Mitchels, and F. Marken, *ChemElectroChem*, **2014**, *1*, 1640-1646.

[10] K. Abe, and H. Kimura, *J. Neurosci.*, **1996**, *16*, 1066-1071.

[11] M.M. Gadalla, and S.H. Snyder, *J. Neurochem.*, **2010**, *113*, 14-26.

[12] X.Z. Zhang, and J.S. Bian, *ACS Chem. Neurosci.*, **2014**, *5*, 876-883.

[13] A.G. Xuan, D.H. Long, J.H. Li, W.D. Ji, M. Zhang, L.P. Hong, J.H. Liu, *J. Neuroinflammation*, **2012**, *9*, 202.

[14] L.F. Hu, M. Lu, C.X. Tiong, G.S. Dawe, G. Hu, and J.S. Bian, *Aging Cell*, **2010**, *9*, 135-146.

[15] K. Song, F. Wang, Q. Li, Y.B. Shi, H.F. Zheng, H. Peng, H.Y. Shen, C.F. Liu, and L.F. Hu, *Kidney Internat.*, **2014**, *85*, 1318-1329.

[16] M. Whiteman, K.M. Gooding, J.L. Whatmore, C.I. Ball, D. Mawson, K. Skinner, J.E. Tooke, A.C. Shore, *Diabetologia*, **2010**, *53*, 1722-1726.

[17] C. Szabo, *Antioxidants Redox Signal.*, **2012**, *17*, 68-80.

[18] M. Whiteman, P.G. Winyard, *Expert Rev. Clin. Pharmacol.*, **2011**, *4*, 13-32.

[19] G.K. Kolluru, X. Shen, S.C. Bir, and C.G. Kevil, *Nitric Oxide-Biol. Chem.*, **2013**, *35*, 5-20.

[20] N.S. Lawrence, J. Davis, L. Jiang, T.G.J. Jones, S.N. Davies, and R.G. Compton, *Electroanalysis*, **2000**, *12*, 1453-1460.

[21] F. Marken, A. Blythe, R.G. Compton, S.D. Bull, and S.G. Davies, *Chem. Commun.*, **1999**, 1823-1824.

[22] N.S. Lawrence, J. Davis, F. Marken, L. Jiang, T.G.J. Jones, S.N. Davies, and R.G. Compton, *Sens. Actuators B-Chem.*, **2000**, *69*, 189-192.

[23] N.S. Lawrence, L. Jiang, T.G.J. Jones, and R.G. Compton, *Anal. Chem.*, **2003**, *75*, 2054-2059.

[24] B. Peng, and M. Xian, *Asian J. Org. Chem.*, **2014**, *3*, 914-924.

[25] C. Liu, J. Pan, S. Li, Y. Zhao, L.Y. Wu, C.E. Berkman, A.R. Whorton, and M. Xian, *Angew. Chem.-Internat. Ed.*, **2011**, *50*, 10327-10329.

[26] H. Peng, Y. Cheng, C. Dai, A.L. King, B.L. Predmore, D.J. Lefer, and B. Wang, *Angew. Chem.-Internat. Ed.*, **2011**, *50*, 9672-9675.

[27] T. Ubuka, T. Abe, R. Kajikawa, and K. Morino, *J. Chrom. B*, **2001**, *757*, 31-37.

[28] J. Furne, A. Saeed, and M. D. Levitt, *Am. J. Physiol.-Regul. Integr. Compar. Physiol.*, **2008**, *295*, R1479-R1485.

[29] N.S. Lawrence, R.P. Deo, and J. Wang, *Anal. Chim. Acta*, **2004**, *517*, 131-137.

[30] B. Spilker, J. Randhahn, H. Grabow, H. Beikirch, and P. Jeroschewski, *J. Electroanal. Chem.*, **2008**, *612*, 121-130.

[31] E.I. Rogers, A.M. O'Mahony, L. Aldous, and R.G. Compton, in D.M. Fox, M. Mizuhata, H.C. DeLong, R.A. Mantz, P.C. Trulove, (eds.), Molten Salts and Ionic Liquids 17, *ECS Transactions*, **2010**, *33*, 473-502.

[32] N.S. Lawrence, L. Jiang, T.G.J. Jones, and R.G. Compton, *Anal. Chem.*, **2003**, *75*, 2499-2503.

[33] N.S. Lawrence, J. Davis, L. Jiang, T.G.J. Jones, S.N. Davies, and R.G. Compton, *Electroanalysis*, **2001**, *13*, 432-436.

[34] G.G. Wildgoose, D. Giovanelli, O.V. Klymenko, N.S. Lawrence, L. Jiang, T.G.J. Jones, and R.G. Compton, *Electroanalysis,* **2004**, *16*, 337-344.

[35] D. Giovanelli, N.S. Lawrence, S.J. Wilkins, L. Jiang, T.G.J. Jones, and R.G. Compton, *Talanta*, **2003**, *61*, 211-220.

[36] V. Aumond, M. Waeles, P. Salaün, K. Gibbon-Walsh, C.M.G. van den Berg, P.-M. Sarradin, R.D. Riso, *Anal. Chim. Acta*, **2012**, *753*, 42– 47.

[37] D. Giovanelli, N.S. Lawrence, L. Jiang, T.G.J. Jones, and R.G. Compton, *Sens. Actuators B-Chem.*, **2003**, *88*, 320-328.

[38] N.L. Whitfield, E.L. Kreimier, F.C. Verdial, N. Skovgaard, and K. R. Olson, *Am. J. Physiol.-Regul. Integr. Compar. Physiol.*, **2008**, *294*, R1930-R1937.

[39] E. Bitziou, M.B. Joseph, T.L. Read, N. Palmer, T. Mollart, M. E. Newton, and J.V. Macpherson, *Anal. Chem.*, **2014**, *86*, 10834-10840.

[40] M.A. Aziz, M. Sohail, M. Oyama, and W. Mahfoz, *Electroanalysis*, **2015**, DOI: 10.1002/elan.201400539.

[41] X. Shen, C.B. Pattillo, S. Pardue, S.C. Bir, R. Wang, and C.G. Kevil, *Free Radical Biol. Med.,* **2011**, *50*, 1021–1031.

[42] A.J. Gross, and F. Marken, *Electroanalysis*, **2015**, *27*, 1035-1042.

[43] F. Marken, J.C. Eklund, and R.G. Compton, *J. Electroanal. Chem.*, **1995**, *395*, 335-339.

[44] R.G. Compton, F. Marken, C.H. Goeting, R.A.J, McKeown, J.S. Foord, G. Scarsbrook, R.S. Sussmann, and A.J. Whitehead, *Chem. Commun.*, **1998**, 1961-1962.

[45] N.S. Lawrence, M. Thompson, C. Prado, L. Jiang, T.G.J. Jones, and R.G. Compton, *Electroanalysis*, **2002**, *14*, 499-504.

[46] F. Marken, C.A. Paddon, D. Asogan, *Electrochem. Commun.*, **2002**, *4*, 62-66.

[47] R.G. Compton, and C.E. Banks, in *Understanding Voltammetry*, Imperial College Press, London, 2007, p. 95.

[48] P. S. Stewart, *J. Bacteriology*, **2003**, *185*, 1485-1491.

[49] M. Whiteman, and P.K. Moore, *J. Cell. Mol. Med.*, **2009**, *13*, 488-507.